

## **COUPLED CFD/FEM ANALYSIS OF MAGNETORHEOLOGICAL FLUID WORN JOURNAL BEARINGS**

**ATHANASIOS K. MICHALOS<sup>\*</sup> AND PANTELIS G. NIKOLAKOPOULOS<sup>\*</sup>**

<sup>\*</sup> Machine Design Laboratory, Mechanical and Aeronautical Engineering. University of Patras, Rio  
Patras, Patras, 26500, Greece.  
e-mail: up1059800@upnet.gr, pnikolakop@upatras.gr

**Abstract.** The current paper discusses the use of magnetorheological fluids (MRFs) for the lubrication of journal bearings as an effective solution for controlling performance – wise a variety of rotor bearing systems applying an external magnetic field. To account for the magnetic flux production in the lubricating layer, a 2D axisymmetric magnetostatic model is developed while the static performance metrics of the journal bearing are assessed via a 3D CFD analysis modeling the MR fluid as a Bingham plastic the rheological parameters of which depend on magnetic field intensity. Moreover, is concluded that MRFs have a wear compensatory feature, increasing the minimum lubricant thickness to a degree that completely compensates possible wear, filling the worn region with high viscosity lubricant.

**Key words:** Journal Bearings, Magnetorheological Fluids, Wear Compensation, CFD/FEM Analysis, Magnetostatic Model, Bingham Plastic.

### **1 INTRODUCTION**

Magnetorheological fluids constitute a sub – category of smart materials that exhibit drastic changes of their rheological properties via excitation by an externally applied magnetic field. This behavior of MR fluids is caused by the induced polarization of micro – sized particles (1 – 100  $\mu\text{m}$ ) in a non – magnetic carrier fluid as a result of the externally applied magnetic field. This allows the fluid to obtain a quasi – solid state within milliseconds, causing the formation of chain – like structures along the magnetic field direction. Because of these structures, the behavior of these fluids is characterized via the Bingham visco – plastic model according to which the MR fluid develops a yield stress and consequently increasing its apparent viscosity.

As a core component of rotating systems, bearings rely their operation highly on the lubrication. However, the ever increasing needs for high efficiency and reliability, higher power density and robustness of rotating machines have focused the interest of many engineers on the idea of active lubrication in order to achieve the optimal operation of rotating systems under any conditions. This can be achieved via the MR fluid lubricated journal bearings by adjusting the magnetic field intensity which consequently alters the viscous properties of the fluid

Because of the unique properties of MR fluids, a major portion of the scientific community has been inspired and many researchers have lately presented designs of magnetorheological devices, such as dampers, clutches, several types of bearings, valves and mountings. Particularly, in the field of MR lubricated journal bearings, Zapomél et al. <sup>[1]</sup> presented an active magnetorheological fluid hydrodynamic bearing. The computational

simulations confirmed that as the magnetic field strength was increasing, the load carrying capability of the journal was also increasing, shifting the eccentricity direction towards the vertical one. Urreta et al. [2] proposed active journal bearings, using a ferrofluid and a MR fluid as lubricants. Bompos and Nikolakopoulos [3] studied a MR lubricated journal bearing and estimated static performance characteristics for various magnetic field intensity values and bearing slenderness ratios. They also conducted a stability analysis of a journal bearing lubricated by magnetorheological (MR) and nano – magnetorheological (NMR) fluids [4]. Wang et al. [5] designed a MR lubricated bearing incorporating a permanent ring neodymium magnet indicating the necessity of magnetic field adjustability for practical application of magnetic fluids in bearings. Lampaert et al. [6] proposed the idea of the rheological texture in a hybrid (Hydrodynamic – Hydrostatic) MR journal bearing operating hydrostatically at low and hydrodynamically at high speeds.

A few researchers have proved that wear presence impacts the dynamic behavior of the bearings themselves also provoking oscillations of the rotating systems. Dufrane et al. [7] studied journal bearings of steam turbines at low speeds and examined the present wear, formulating two wear models. The former considers that the journal is imprinted on the bearing, while the latter considers that the worn arc radius is higher than that of the journal. Hashimoto et al. [8] studied the influence of wear presence on hydrodynamic bearings in laminar and turbulent regimes. Fillon and Bouyer [9] analyzed worn journal bearings taking into account also temperature variation indicating that the worn region is possible to induce the generation of a secondary pressure peak just like a multistep journal bearing. Machado et al. [10] created a numerical model of a worn journal bearing to examine the wear impact on the dynamic response of rotating systems in frequency domain. Gertzog et al. [11] devised a generic method for remote identification of the wear depth utilizing measurements relatively to the bearing's operating condition and for prediction of the wear depth progress via Archard's abrasive wear model.

In the current paper a coupled simulation of a MR fluid journal bearing takes place, using ANSYS software package. The magnetic field is resolved via a 2D axisymmetric magnetostatic model, while the flow field via a 3D CFD analysis considering the MR fluid as a Bingham plastic in CFX solver of ANSYS. The originality of the paper lies in the use of MR fluids also in the case of worn journal bearings and their ability of wear compensation is examined. In conclusion, journal bearing performance parameters and particularly load carrying capacity, attitude locus and friction coefficients are derived and presented for several aspect ratios, values of magnetic field intensity and in the case of wear, for several wear depths as functions of dimensionless Sommerfeld number.

## 2 THEORETICAL BACKGROUND

### 2.1 Geometrical model of worn journal bearing

For the purpose of the current work, a steady, laminar and isothermal flow field is considered inside the bearing domain neglecting bearing's possible deformations. The geometry of a worn bearing is shown in Fig. 1a. Although the external load  $W$  is vertical, the journal does not deflect co – directionally with the load but instead always moves at an angle to the load – line and balances when the total hydrodynamic force  $F_h$  equals the external load  $W$ . This angle is known as attitude angle, symbolized as  $\varphi$  in Fig. 1, and is given by:  $\varphi = \arctan(F_t/F_r)$ , where  $F_t$ ,  $F_r$  are the load components perpendicular and parallel to the

eccentricity direction. Finally, MR fluid flows between the journal and the bearing which is activated when a magnetic field is applied into it.

By defining a coordinate system relative to the eccentricity direction (see Fig. 1), the lubricant film distribution  $h$  in the intact region is extracted:

$$h(\theta) = c_r + e \cos \theta \quad (1)$$

where  $c_r$  is the radial clearance and equals to the concentric distance between journal and bearing.

In the case of worn bearings, the used wear model is the same with that presented by Dufrane et al. [7] who made the observation that the wear pattern is symmetrically positioned with respect to the vertical axis of the bearing and is uniform over the bearing length, as depicted in Fig. 1a. They proposed that the worn region has a radius that is greater than the journal and the distribution of wear depth  $d$  is given by:

$$d = d_0 - c_r \{1 + \cos(\theta + \varphi)\} \quad (2)$$

where  $d_0$  is the maximum wear depth.

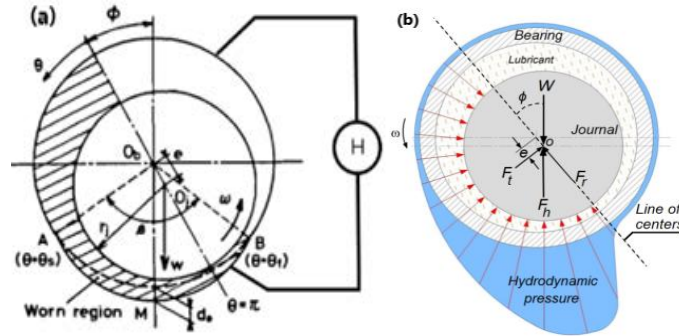


**Figure 1:** (a) Geometry of worn MRF journal bearing, (b) load components and pressure profile of bearing

Adding by terms eq. (1), (2) the following lubricant film distribution in the worn area  $h_w$  is extracted:

$$h_w(\theta) = d_0 + e \cos \theta - c_r \cos(\theta + \varphi) \quad (3)$$

Equating eq. (1), (3) and because the wear pattern is symmetric the angular wear extent  $\beta$  can be calculated as follows:

$$\cos(\pi - \beta/2) = (d_0/c_r) - 1 \quad (4)$$

Finally, the film thickness distribution in the whole fluid domain is given by the following two – branch function:

$$\begin{aligned} h(\theta) &= h_w = d_0 + e \cos \theta - c_r \cos(\theta + \varphi), \quad \theta_s \leq \theta \leq \theta_f \\ h(\theta) &= c_r + e \cos \theta, \quad \theta < \theta_s, \theta > \theta_f \end{aligned} \quad (5)$$

## 2.2 Description of magnetostatic model

The magnetostatic analysis was conducted based on a model similar to that proposed by Zapomêl et al. [1]. The bearing housing is practically an axisymmetric E – shaped section (see

Fig. 2) resulting in a hollow rotor journal. The annular domain between the surfaces of the bearing housing and the shaft journal is filled with MR fluid. The bearing housing's whole body is constructed of a magnetically permeable material, whereas the hollow journal shaft is made of magnetically non - conductive material to prevent magnetic interaction with the bearing housing body.

In order to generate a magnetic field in the lubricant layer, an electrical coil is wound around the cylindrical part of the bearing housing, producing a magnetic flux path through all key components as shown in the below schematic diagram of Fig. 2.

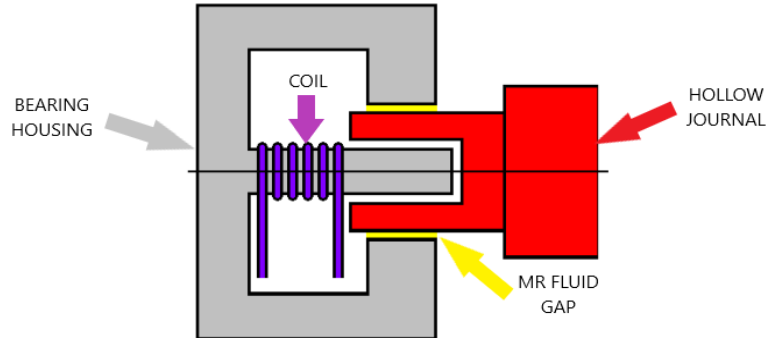


**Figure 2:** Schematic diagram of bearing housing

From the material assignment of the parts of the magnetostatic model, it can be assumed that magnetic reluctance of the bearing housing is negligible than that of the MR fluid gap or the air gap between the journal and the cylindrical part of the housing. Therefore, Hopkinson law can be applied in order to calculate magnetic flux density in the lubricant layer according to which:

$$\frac{\Phi_S}{S_S} = \mu_0 N_C \frac{I}{R - R_C} \quad (6)$$

where  $\Phi_S$  the magnetic flux through the magnetic core,  $S_S$  the cross sectional area of the bearing housing,  $\mu_0$  the permeability of vacuum,  $N_C$  the number of coil turns,  $I$  the applied current,  $R$  is the bearing radius and  $R_C$  is the cylindrical part radius.

Furthermore since the width of the MR fluid gap is in the order of  $\mu\text{m}$ , the magnetic flux in the lubricant layer remains unaffected by the journal's movement relative to the bearing bushing.

### 2.3 Rheological behavior of MR fluids

As already mentioned, MR lubricants act like Newtonian fluids in the absence of magnetic field while they show a magnetically dependent yield stress when magnetic field is present, in which case the magnetically induced particles are orientated with respect to the magnetic field direction.

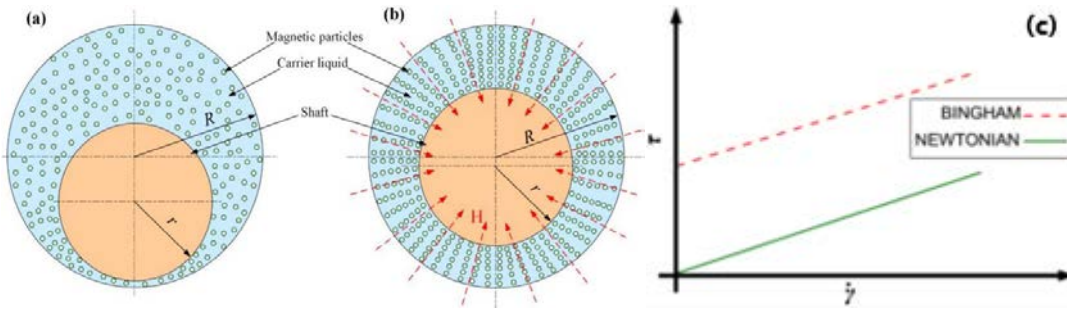


**Figure 3:** Distribution of magnetic particles (a) without, (b) with magnetic field in a journal bearing, (c) Bingham plastic model

MR fluids can be rheologically characterized by the Bingham plastic model (see also Fig. 3c) according to which when shear stress overcomes a critical value, named yielding shear stress ( $\tau_0$ ), the MR fluid starts to flow. The innovative characteristic behind MR fluids is that yield stress depends on the current value of magnetic intensity  $H$ , a relation that may be inferred from experimental or manufacturer's data for commercial MR fluids.

## 2.4 Governing equations of flow field

The second part of this coupled simulation concerns the flow field analysis of the MR fluid inside the eccentric annulus domain between the journal and the bearing. The studied fluid flow is considered steady – state, laminar and isothermal and therefore only the conservation equations of mass and momentum are necessary.

The continuity equation for the above flow type is as follows:

$$\nabla \cdot (\vec{u}) = 0 \quad (9)$$

where  $\vec{u}$  the fluid velocity vector.

Momentum conservation for the particular flow type is described by:

$$\rho \nabla \cdot (\vec{u}\vec{u}) = -\nabla p + \nabla \cdot (\vec{\tau}) + \rho \vec{g} + \vec{F} \quad (10)$$

where  $\rho$  the fluid density,  $p$  the static pressure,  $\rho \vec{g}$  the gravitational body force and  $\vec{F}$  the external body force from the applied magnetic field.

In the end, the stress tensor  $\vec{\tau}$  is given by:

$$\vec{\tau} = \mu_a \left[ (\nabla \vec{u} + (\nabla \vec{u})^T) - \frac{2}{3} \nabla \cdot \vec{u} \vec{I} \right] \quad (11)$$

where the term  $\frac{2}{3} \nabla \cdot \vec{u} \vec{I}$  expresses the fluid volume dilation.

## 3 SIMULATION SETUP

### 3.1 Magnetostatic model

For the magnetostatic analysis of the bearing housing, Magnetostatic module of ANSYS Workbench was used, analyzing the whole configuration as a 2D axisymmetric model (see Fig. 4). For a given applied current to the electrical coil, the magnetic induction and field intensity

at the MR fluid can be determined.

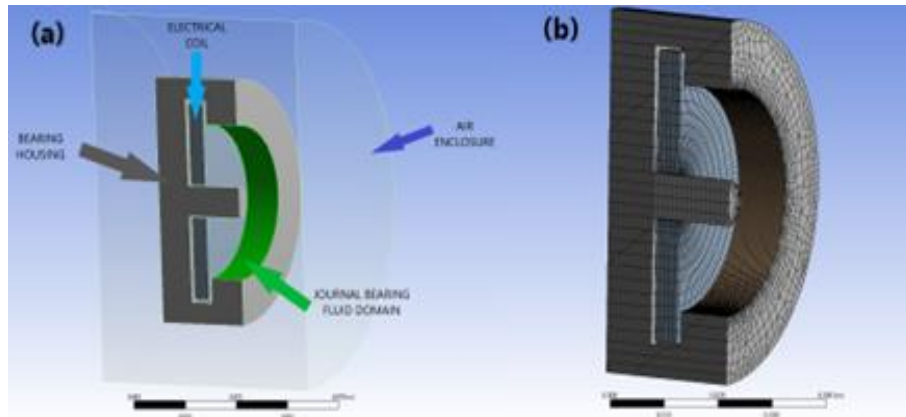


**Figure 4:** (a) The 2D axisymmetric magnetostatic model of a narrow journal bearing ( $L/D = 1/4$ ) in ANSYS 16.0 and (b) its discretization mesh

The material assignment of the structures of the whole configuration was done via predefined ANSYS material libraries. Particularly, the bearing housing is made of gray cast iron, a common material for the construction of iron cores and the electrical coil is made of copper alloy. Inside the fluid domain flows the MR fluid MRF-132 DG provided by Lord Corp., while for the magnetostatic analysis its  $B - H$  curve was used in order to define the journal bearing fluid domain<sup>[12]</sup>.

The magnetostatic simulation demands a fairly high discretization and for this reason a structured mesh of relatively high accuracy is required specifically of the fluid domain, the electrical coil and the cross section area of the bearing housing. Most notably, the discretization of the fluid domain includes 360 circumferential divisions and an element size of 0.5 mm was used in the axial direction, while for this kind of simulation film thickness discretization is not needed. The mesh has relevance value of 50 and consists of 483912 elements and 824040 nodes.

In all magnetostatic simulations the coil has 600 turns and its area remains constant, determining the magnetic flux density at the MR fluid at various input DC current values from 200 mA to 3A. Therefore, the yield stress  $\tau_0$  of the MR fluid can be determined via the  $\tau_0 - H$  curve of the MR fluid, which is extracted experimentally or in this case by manufacturer's data<sup>[12]</sup>. The air enclosure is set as a zero magnetic potential boundary condition, practically isolating the current magnetostatic model from the surrounding space.

### 3.2 CFD model

The flow field was solved with the CFX solver of ANSYS suite, solving the mass conservation and 3D Navier – Stokes equations. The geometry model is the same with that presented in Fig. 2.

The discretization mesh was created using hexahedral elements distributed as follows: 360 circumferential divisions, 50 axial dimensions and 25 divisions in the direction of lubricant film thickness. The mesh in total consisted of 477360 nodes and 450000 elements.

As boundaries conditions, the bearing surface is set as a stationary wall while the journal surface as a rotating wall that rotates at 1500 rpm around the respective axis of rotation. As for

the two peripheral surfaces of the fluid domain, they constitute the inlet and outlet of the lubricant defined within the software as “openings” with zero relative pressure in order to prevent possible backflow.

The MR fluid used in the simulations is the MRF-132 DG provided by Lord Corp.<sup>[12]</sup>. Lastly, the values of minimum and maximum shear strain rate for the MR fluid are set to  $10^{-6}$  and  $10^6 \text{ s}^{-1}$  respectively while the convergence residual is the same for all conservation equations and equal to  $10^{-6}$  (RMS value).

### 3.3 Journal equilibrium position

The geometric description of the journal bearing requires the estimation of the journal equilibrium point, by determining the attitude angle relatively to the current eccentricity (see Fig. 1a). For this purpose, a MATLAB script was written to be able to numerically solve the generalized Reynolds equation through the Finite – Difference approach. With the necessary bearing / lubricant properties, the fluid domain is transformed to a discretized cartesian plane at the nodes of which the pressure distribution values are determined until the respective convergence criteria is met. Then, the total load force and its components are calculated by integrating numerically pressure distribution and the attitude angle is obtained. For worn journal bearings, there is a second iterative loop because eq. (5) is a function of the desired attitude angle and therefore an initial value of it must be considered until the convergence criteria is met. This procedure is also presented by the following flow chart:

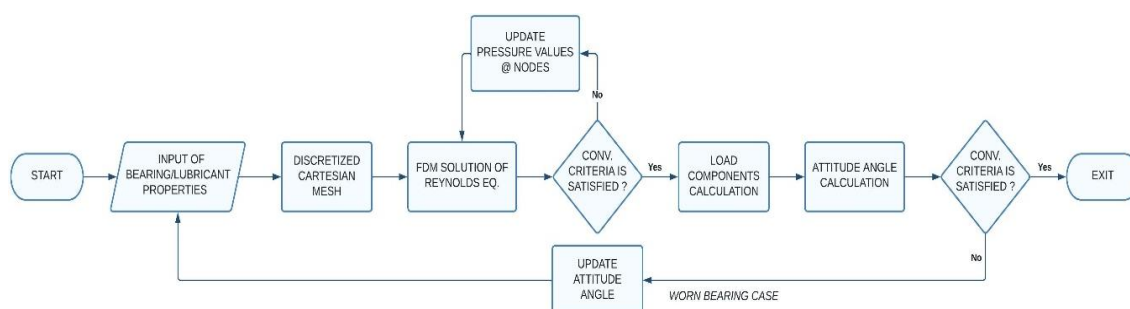


**Figure 5:** Flow chart of journal equilibrium sub - problem

## 4 RESULTS

### 4.1 Magnetostatic case results

In Fig. 6 the magnetic induction and magnitude of magnetic field intensity in the lubricant domain are presented as functions of the applied current. The following results are verified by the findings of Zapomél et al.<sup>[1]</sup> and confirm that the induced magnetic field does not depend greatly on the aspect ratio ( $L/D$ ) of the journal bearing while the journal displacement does not affect neither the intensity nor the uniformity of the magnetic field.



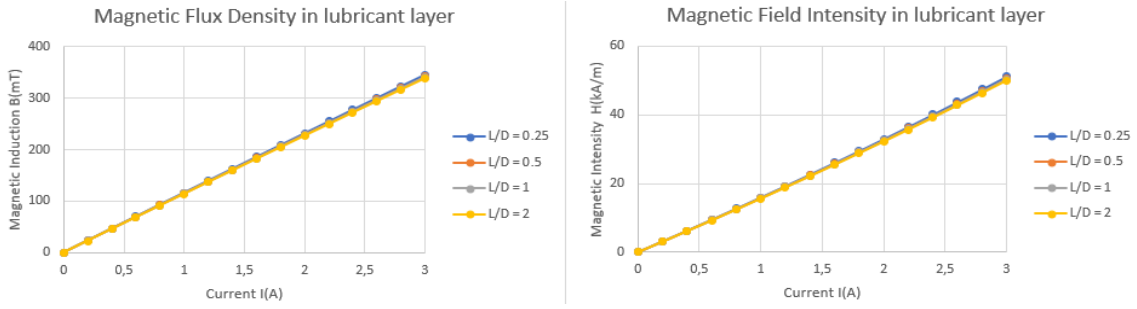


**Figure 6:** Magnetic induction and magnitude of magnetic field intensity in the lubricant layer as functions of the applied current

## 4.2 CFD case results of intact journal bearings

In general, the CFD results concern the use of Newtonian and MR (Bingham) lubricant for bearing aspect ratios  $L/D = 1/4, 1/2, 1, 2$ . Defining the dimensionless yield stress as  $T_0 = \tau_0 c_r / \mu \omega R_j$  for the case of Bingham lubricant, results are also presented for three cases of  $T_0 = 0.4, 0.8, 1.2$ . The Newtonian case results are compared and validated to the ones of Raimondi and Boyd<sup>[13]</sup> for  $L/D = 1/4, 1/2, 1, \infty$  while the Bingham case ones to those of Wada et al.<sup>[14]</sup>

The results of Fig. 7 show the reduction of Sommerfeld number with of presence MR fluid ( $T_0 = 1.2$ ). For  $L/D = 0.25$ , load carrying capacity increases by 24.6% - 36.5% ( $\varepsilon = 0.15 - 0.96$ ) while for  $L/D = 2$ , increases by 7.64% - 28.7% ( $\varepsilon = 0.16 - 0.87$ ) indicating the lower influence of the MR fluid in longer journal bearings. Also, the eccentricity ratio decreases as  $L/D$  ratio increases in both Newtonian and Bingham cases with constant Sommerfeld number.

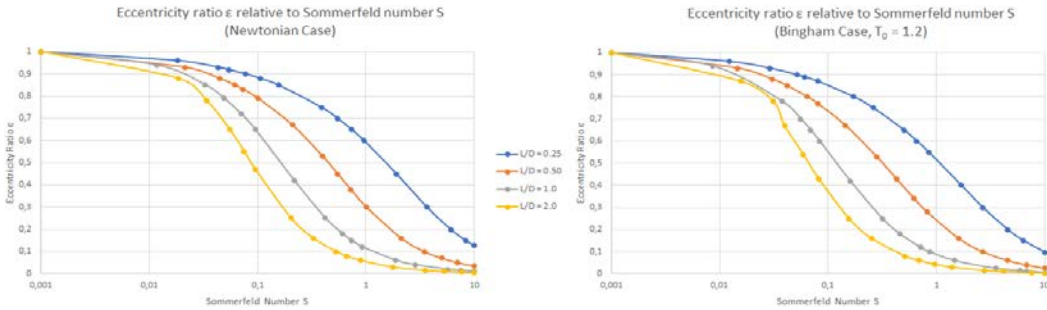


**Figure 7:** Eccentricity ratio  $\varepsilon$  ( $e/c_r$ ) versus Sommerfeld number for intact journal bearing

As it can be seen from Fig. 8 friction coefficients increase with an increase of the dimensionless yield stress  $T_0$  (here:  $T_0 = 1.2$ ) under the same Sommerfeld number. For  $L/D = 0.25$  journal friction coefficient is increased by 0.790% - 21.4% ( $\varepsilon = 0.23 - 0.94$ ), while bearing one is increased by 1.11% - 22.5% for the same eccentricity ratio range. For  $L/D = 2$  journal friction coefficient is increased by 5.98% - 68.15% ( $\varepsilon = 0.16 - 0.82$ ), while bearing one is increased by 16.3% - 70.5% for the same eccentricity ratio range. It seems that the effect of the MR fluid is much greater in long journal bearings. Furthermore, the bearing friction coefficient is lower than the respective journal one, a trend that become more prominent as the Sommerfeld number decreases.



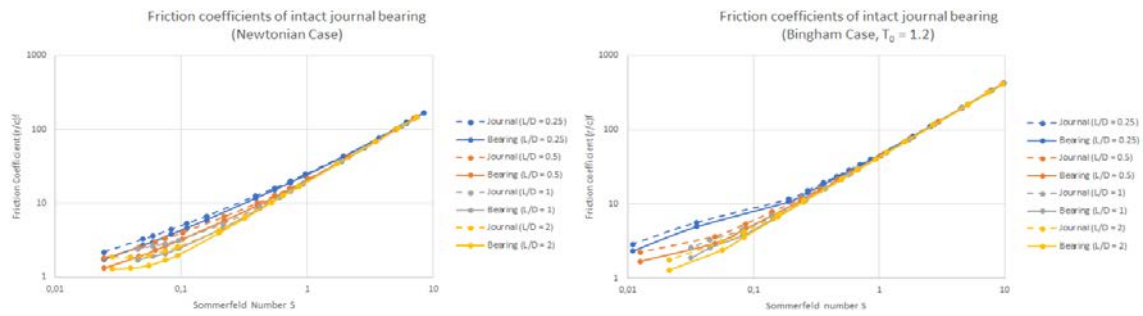


**Figure 8:** Friction coefficients at surfaces of intact journal bearing

Fig. 9 shows the attitude locus of the journal ( $T_0 = 1.2$ ). According to the corresponding diagrams, on the one hand higher load conditions result in reduction of attitude angle and on the other attitude angle increases with increment of current intensity. For  $L/D = 0.25$ , the increment ranges from 0.324% - 4.70% ( $\varepsilon = 0.15 - 0.96$ ). For  $L/D = 2$ , ranges from 0.854% - 4.55% ( $\varepsilon = 0.16 - 0.87$ ), indicating practically same behavior in both cases.

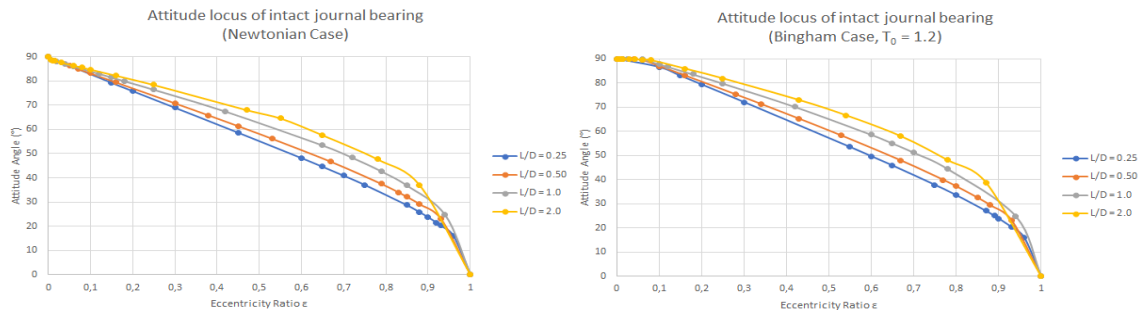


**Figure 9:** Attitude locus of intact journal bearing

### 4.3 CFD case results of worn journal bearings

For the purpose of the wear cases, a journal bearing with  $L/D = 1$  was considered lubricated by Newtonian and MR fluid. Defining the wear depth ratio  $\delta$  as the ratio of the maximum wear depth to the radial clearance, results were extracted for two wear depth ratios  $\delta = 0.25, 0.5$  and three cases of  $T_0 = 0.4, 0.8, 1.2$ . The results were compared and validated to the theoretical ones presented by Hashimoto et al. [8] for  $\delta = 0.5$  for an eccentricity ratio range 0.3 – 0.93.

In Fig. 10 the relation between eccentricity ratio and dimensionless Sommerfeld number is presented ( $T_0 = 1.2$ ). In the case of wear depth  $\delta = 0.25$  load carrying capacity increases by 36.0% - 42.3% and in the case of wear depth  $\delta = 0.5$  increases by 35.8% - 41.8% ( $L/D = 1, \varepsilon = 0.3 - 0.93$ ) presenting the wear compensatory feature of MR fluids. Moreover, the load capacity increment is reduced by  $\approx 1\%$  for an eccentricity ratio step of 0.1.

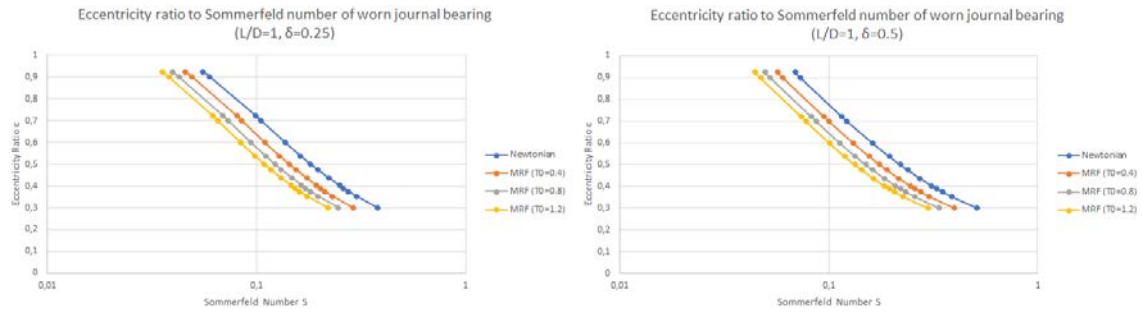


**Figure 20:** Eccentricity ratio  $\varepsilon$  ( $e/c_r$ ) versus Sommerfeld number for worn journal bearing

In Fig. 11 the friction coefficients at both surfaces of the journal bearing are shown ( $T_0 = 1.2$ ). The friction coefficients on bearing and journal surfaces both increase, while the increment percentage is lowered by increasing the eccentricity ratio. For  $\delta = 0.25$  journal friction coefficient is increased by 6.92% - 28.0% and the bearing one by 9.01% - 28.9% ( $L/D = 1$ ,  $\varepsilon = 0.3 - 0.93$ ). For  $\delta = 0.5$  journal friction coefficient is increased by 14.0% - 28.0% while bearing one is increased by 0.954% - 26.2% for the same  $L/D$  ratio and eccentricity ratio range. Similarly to the case of intact journal bearings, the bearing friction coefficient is lower than the journal one specifically for lower Sommerfeld number values.

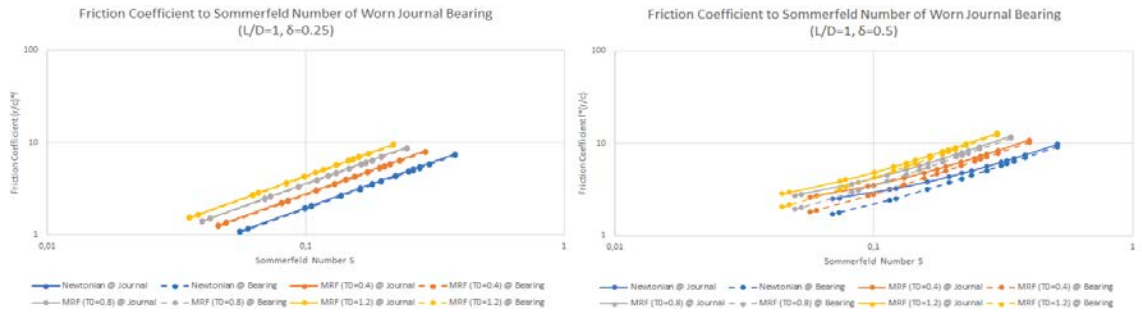


**Figure 31:** Friction coefficients at the surfaces of worn journal bearing

In conclusion, Fig. 12 shows the attitude locus of a worn journal bearing for two wear depth scenarios  $\delta = 0.25, 0.5$  ( $T_0 = 1.2$ ). It can be seen that higher wear depth ratio results in lower attitude angle values. The effect of MR fluid causes the attitude angle to decrease up until  $\varepsilon \approx 0.7$  and then increases. For  $\delta = 0.25$ , the decrement range is 0.850% - 2.36% and the increment range reaches to 2.13%. For  $\delta = 0.5$ , the decrement range is 1.22% - 2.52% while the increment one reaches higher to 6.93%.

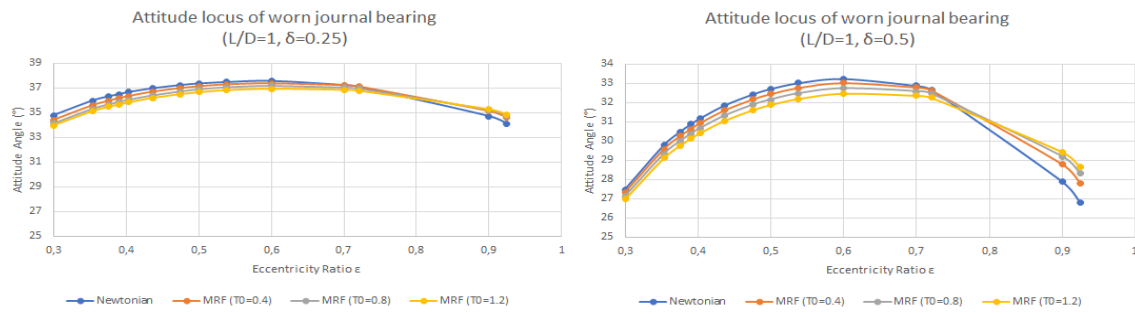


**Figure 42:** Attitude locus of worn journal bearing

## 5 SUMMARY

The steady – state behavior of a MRF lubricated worn journal bearing was examined via coupled Magnetostatic – 3D CFD simulations in ANSYS Suite. Significant importance was given in the magnetostatic model and its structure to ensure the creation of a radially uniform magnetic field in the MR fluid. Then, the rheological model is solved by CFX solver of ANSYS and the above results are presented in convenient diagrams for further design of such smart journal bearings.

The use of MR fluid lubricated journal bearings seems to be a promising application relatively to their beneficial performance characteristics and their controllability also under the presence of wear. Future research should be focused on the structural optimization of such structures in terms of energy cost optimization and on their operation with active, closed loop systems to ensure their optimum performance under any required conditions and wear intensity.

## REFERENCES

- [1] J. Zapomêl and P. Ferfecki, "A new concept of a hydrodynamic bearing lubricated by composite magnetic fluid for controlling the bearing load capacity," *Mechanical Systems and Signal Processing*, vol. 168, 1 April 2022.
- [2] H. Urreta, Z. Leicht, A. Sanchez, A. Agirre, P. Kuzhir and G. Magnac, "Hydrodynamic Bearing Lubricated with Magnetic Fluids," *Journal of Physics: Conference Series*, vol. 149, 14 December 2009.
- [3] D. A. Bompos and P. G. Nikolakopoulos, "CFD simulation of magnetorheological fluid journal bearings," *Simulation Modelling Practice and Theory*, vol. 19, no. 4, pp. 1035-1060, 1 April 2011.
- [4] D. A. Bompos and P. G. Nikolakopoulos, "Journal Bearing Stiffness and Damping Coefficients Using Nanomagnetorheological Fluids and Stability Analysis," *Journal of Tribology*, vol. 136, no. 4, 19 June 2014.
- [5] A. Wang, J. Pan, H. Wu and J. Ye, "Structural Design and Lubrication Properties under Different Eccentricity of Magnetic Fluid Bearings," *Applied Sciences*, vol. 12, no. 14, 2022.
- [6] S. G. Lampaert, F. Quinci and R. A. van Ostayen, "Rheological texture in a journal bearing with magnetorheological fluids," *Journal of Magnetism and Magnetic Materials*, vol. 499, 1 April 2020.
- [7] K. F. Dufrane, J. W. Kannel and T. H. McCloskey, "Wear of steam turbine journal bearings at low operating speeds," *Journal of Lubrication Tecnology*, vol. 105, pp. 313-317, 1983.
- [8] H. Hashimoto, S. Wada and K. Nojima, "Performance Characteristics of Worn Journal Bearings in Both Laminar and Turbulent Regimes. Part I: Steady-State Characteristics," *ASLE TRANSACTIONS*, vol. 29, no. 4, pp. 565-571, 1986.
- [9] M. Fillon and J. Bouyer, "Thermohydrodynamic analysis of a worn plain journal bearing," *Tribology International*, vol. 37, no. 2, pp. 129-136, 1 February 2004.
- [10] T. H. Machado and K. L. Cavalca, "Modeling of hydrodynamic bearing wear in rotor-bearing systems," *Mechanics Research Communications*, vol. 69, pp. 15-23, 1 October 2015.
- [11] K. Gertzog, P. Nikolakopoulos, A. Chasalevris and C. Papadopoulos, "Wear identification in rotor-bearing systems by measurements of dynamic bearing characteristics," *Computers & Structures*, vol. 89, no. 1, pp. 55-66, 1 January 2011.
- [12] "MRF-132 DG Magnetorheological Fluid Technical Data," Cary NC, Cary NC, 2011.
- [13] A. A. Raimondi and J. Boyd, "A solution for the finite journal bearing and its application to analysis and design: III," *ASLE Transactions*, vol. 1, pp. 194-209, 1958.
- [14] S. Wada, H. Hayashi and K. Haga, "Behavior of Bingham Solid in Hydrodynamic Lubrication Part 3. Application to Journal Bearing," *Bulletin of the JSME*, vol. 17, no. 111, pp. 1182-1191, September 1974.